A novel nematode species from the Siberian permafrost shares adaptive mechanisms for cryptobiotic survival with *C. elegans* dauer larva

Anastasia Shatilovich[1#], Vamshidhar R. Gade[2,9#], Martin Pippel[3], Tarja T. Hoffmeyer[4], Alexei V. Tchesunov[5], Lewis Stevens[6], Sylke Winkler[2,7], Graham M. Hughes[8], Sofia Traikov[2], Michael Hiller[3,10], Elizaveta Rivkina[1], Philipp H. Schiffer[4*], Eugene W Myers[3], Teymuras V. Kurzchalia[2*]

1. Institute of Physicochemical and Biological Problems in Soil Science RAS, Pushchino, Russia
2. Max Planck Institute for Molecular Cell Biology and Genetics, Dresden, Germany
3. Center for Systems Biology, Dresden, Germany
4. Institute for Zoology, University of Cologne
5. Department of Invertebrate Zoology, Faculty of Biology, M.V. Lomonosov Moscow State University, Moscow, Russia
6. Tree of Life, Wellcome Sanger Institute, Cambridge, UK
7. DRESDEN concept Genome Center, Dresden, Germany
8. School of Biology and Environmental Science, University College Dublin, Belfield, Dublin, Ireland
9. Institute of Biochemistry, ETH Zürich, 8093 Zürich, Switzerland
10. LOEWE Centre for Translational Biodiversity Genomics, Senckenberg Society for Nature Research & Goethe University, Frankfurt am Main, Germany

[#] A.S and V.G contributed equally to this work

*To whom correspondence may be addressed

Email: kurzchalia@mpi-cbg.de

p.schiffer@uni-koeln.de

Abstract

Some organisms in nature have developed the ability to enter a state of suspended metabolism called cryptobiosis[1] when environmental conditions are unfavorable. This state-transition requires execution of genetic and biochemical programs[1,2,3] that enables the organism to survive for prolonged periods. Recently, nematode individuals have been reanimated from Siberian permafrost after remaining in cryptobiosis. Preliminary analysis indicates that these nematodes belong to the genera *Panagrolaimus* and *Plectus*[4]. Here, we present precise radiocarbon dating indicating that the *Panagrolaimus* individuals have remained in cryptobiosis since the late Pleistocene (~46,000 years). Phylogenetic inference based on our genome assembly and a detailed morphological analysis demonstrate that they belong to an undescribed species, which we named *Panagrolaimus n. sp*. Comparative genome analysis revealed that the molecular toolkit for cryptobiosis in *Panagrolaimus n. sp.* and in *C. elegans* is partly orthologous. We show that biochemical mechanisms employed by these two species to survive desiccation and freezing under laboratory conditions are similar. Our experimental evidence also reveals that *C. elegans* dauer larvae can remain viable for longer periods in suspended animation than previously reported. Altogether, our findings demonstrate that nematodes evolved mechanisms potentially allowing them to suspend life over geological time scales.

Introduction

Organisms from diverse taxonomic groups can survive extreme environmental conditions, such as the complete absence of water or oxygen, high temperature, freezing, or extreme salinity. The survival strategies of such organisms include a state known as suspended animation or cryptobiosis, in which they reduce metabolism to an undetectable level[6]. Spectacular examples of long-term cryptobiosis include a *Bacillus* spore that was preserved in the abdomen of bees buried in amber for 25 to 40 million years[7], and a 1000 to 1500 years-old *Lotus* seed, found in an ancient lake, that was subsequently able to germinate[8]. Metazoans such as tardigrades, rotifers and nematodes are also known for remaining in cryptobiosis for prolonged periods[9,10]. The longest records of cryptobiosis in nematodes are reported for the Antarctic species *Plectus murrayi*[11] (25.5 years in moss frozen at -20°C), and *Tylenchus polyhypnus*[12] (39 years desiccated in a herbarium specimen).

Intensive research during the last decades has demonstrated that permafrosts (perennially frozen sediments) are unique ecosystems preserving life forms at sub-zero temperatures over thousands of years[13,14,15,16]. Permafrost remains are an exceptional source for discovering a wide variety of unicellular and multicellular living organisms surviving in cryptobiosis for prolonged periods[6,17,18]. We recently reanimated soil nematodes that were preserved in Siberian permafrost for potentially thousands of years, and initial morphological observations provisionally described them as belonging to the genera *Panagrolaimus* and *Plectus.* Previous studies demonstrated several species of *Panagrolaimus* can undergo cryptobiosis in the form of anhydrobiosis (through desiccation) and cryobiosis (through freezing)[19,20,21,22,23]. In various nematodes, entry into anhydrobiosis is often accompanied by a preparatory phase of exposure to mild desiccation, known as preconditioning[21,24]. This induces a specific remodelling of the transcriptome, the proteome, and metabolic pathways that enhances survival ability[2,3,25]. Some panagrolaimids possess adaptive mechanisms for rapid desiccation where most of the cellular water is lost, while others possess freezing tolerance, without loss of water, at sub-zero temperatures by inhibiting the growth and recrystallisation of ice crystals[21].

Here we present a high-quality genome assembly, detailed morphological phylogenetic analysis, and define a novel species, *Panagrolaimus n. sp.* Precise radiocarbon dating indicates that *Panagrolaimus n. sp* remained in cryptobiosis for about 46,000 years, since late Pleistocene. Furthermore, making use of the model organism *C. elegans*, we demonstrate that *C. elegans* dauer larvae and *Panagrolaimus* utilize comparable molecular mechanisms to

survive extreme desiccation and freezing, i.e. upregulation of trehalose biosynthesis and gluconeogenesis.

Results

Discovery site and radiocarbon dating

Previously, we showed that nematodes from the Siberian permafrost with morphologies consistent with the genera *Panagrolaimus* and *Plectus* could be reanimated thousands of years after they had been frozen in the permafrost. Several viable nematode individuals were found in two out of more than 300 studied samples of permafrost deposits of different ages and genesis, collected by researchers of the Soil Cryology Lab, Pushchino, Russia, during perennial paleo-ecological expeditions carried out in the coastal sector of the northeastern Arctic[17]. The detailed description of the study site (outcrop Duvanny Yar, Kolyma River, Fig.1A), sampling and revitalizing procedures are provided in Supplementary Information (SI). Like other late Pleistocene permafrost formations in the northeastern Arctic, Duvanny Yar comprises permanently frozen ice-rich silt deposits riddled with large polygonal ice wedges and divided by them into mineral blocks[26,27] (Fig.1B). The sediments include sandy alluvial layers, peat lenses, buried paleosols and Pleistocene rodent burrows (Fig.1C). The burrow (P-1320), in which *Panagrolaimus* nematodes were found (Fig.1D), has been taken from the frozen outcrop wall at a depth of about 40 m below the surface and about 11 m above river water level in undisturbed and never thawed late Pleistocene permafrost deposits. The fossil burrow left by arctic gophers of the genus *Citellus* consists of entrance tunnel and a large nesting chamber up to 25 cm in diameter[26].

The sterility of permafrost sampling and age of cultivated biota were discussed in detail in several reviews[14,28, 29]. Based on previous reports, the age of the organisms found in a burrow is equal to the freezing time and corresponds to the age of organic matter conserved in the syncryogenic sediments. This makes it possible to use radiocarbon dating of organic matter to establish the age of organisms. We performed Accelerator Mass Spectrometry (AMS) radiocarbon analysis of plant material obtained from studied borrow P-1320 and determined a direct ^{14}C age of 44,315±405 BP (Institute of Geography, RAS; sample $IGAN_{AMS}$ 9137). Calibrated age range is 45,839 – 47,769 cal BP (95.4% probability) (Fig.S1).

Like other parthenogenetic *Panagrolaimus* the newly discovered species is triploid

The revived animal was cultivated in the laboratory for over 100 generations and initially described as *Panagrolaimus* aff. d*etritophagus*[4] based on morphology. We conducted a detailed morphological analysis of the revived animal (Fig.2, S2, Table S1; BOX1), which confirmed unambiguously that the animal belongs to the genus of *Panagrolaimus*, in agreement with a previous phylogenetic analysis of the 18S ribosomal RNA sequence[4]. However, due to the morphological uniformity of *Panagrolaimus*, unusual even for nematodes, morphology and molecular analysis of a single ribosomal RNA sequence is insufficient to describe a species. We found the species to be parthenogenetic, which further complicates description under most species concept.

To obtain comprehensive molecular data for species determination using phylogenomics, we generated a genome assembly. Using PacBio HiFi sequencing, we generated 84X coverage in long reads (average length 14,425 bp). Our analysis of repeat and gene content is described in Supplementary Table 3. K-mer analysis of the reads clearly indicated that this animal has a triploid genome (Fig.3A), like other parthenogenetic *Panagrolaimus* species[30]. Despite the challenges that a triploid genome poses for assembly, we obtained a highly-contiguous contig assembly of the three pseudohaplotypes that comprise about 266 Mb and thus have a similar genome size as other parthenogenetic *Panagrolaimus* species[30]. The contig N50 value of all three pseudohaplotypes is 3.8 Mb. Since the three pseudohaplotypes exhibited a noticeable degree of divergence, we further investigated their relationship by using the apparent homeologs in our gene predictions to align the longest continuous contigs based on micro synteny (Fig. 3B). Links between the contigs clearly show the triploid state of the genome.

163 **BOX 1 Description of *Panagrolaimus n. sp* sp. nov.**

Description	Body spindle-shaped and usually almost straight after fixation (Fig.2a, b). Cuticle thin and faintly annulated, 10–11 annules per 10 µm in cervical region, 13–14 in midbody, preanally again 10 annules within 10 µm. Conspicuous convex lateral fields with three incisures 1.5-2 µm wide extended along the body from about ¼–1/3 procorpus length to 2/3 of tail length. In SEM, the lateral field looks as a bolster with a narrow median split. Labial region set off. Mouth opening surrounded with six lips (Fig.2c, d). Anterior sensilla as papillae arranged in two close but separate subsequent circles. Somatic sensilla (i.e., deirids and phasmids) not evident. Buccal cavity cylindro-conoid, and unarmed; its total length 9–13 µm, maximum stoma width 1.7–2.8 µm (Fig.2e). Dorsal stoma wall (dorsal rhabdion) more clearly sclerotized. Anterior part of the buccal cavity comprising cheilostom and gymnostom nearly cylindroids while stegostom conically narrowed and ended with a distinct tight flexion. Pharynx consists of three distinct parts: straight anterior procorpus, narrow medial isthmus and rounded terminal bulb. Procorpus gradually widening to it posterior end, always straight in all specimens, with transversal muscular striation, more prominent in posterior three fourths. Isthmus narrow, cylindroid, bent starkly in nearly all studied specimens. Terminal bulb strongly muscular, with a valvular apparatus at about 40% of the bulb length. Cardia in shape of truncate cone. Intestine (midgut) tissue filled with vacuoles and granules; in the anteriormost region, the granules smaller and look more pallid. Cell borders not visible in the intestine, but internal lumen distinct, sinusoid. No internal content visible in the internal lumen. Ventral excretory-secretory pore and its cuticularized duct situated at the level of anterior part of the bulb. No other details of the excretory-secretory system visible. Vulval lips protruding. Genital branch monodelphic prodelphic and situated dorsally and to the right of the midgut (Fig.2f). Vagina distinctly cuticularized and opens to the elongate uterus. A long oviduct extended anteriad from the anterior uterus; the oviduct folded up and then posteriorward and transforms into an elongate ovary. There are

	one or two ripe eggs in the uterus in most specimens. Tail short conical, with short acute spike-like mucro (Fig.2g).
Etymology	Species name *kolymaensis* (Latin) is derived from the Kolyma River area.
Holotype	Senckenberg Natural History Museum, Frankfurt am Main, Germany (collection number SMF 17067).
Paratypes	Senckenberg Natural History Museum, Frankfurt am Main, Germany (collection numbers SMF 17068, SMF 17069) (eighteen paratypes).
Type locality	Frozen fossil rodent burrow buried in permafrost 45,839 – 47,769 cal BP, 40 meters from the surface, outcrop Duvanny yar, Kolyma River, North-East of Siberia, Russia (68.633410, 159.078800). Frozen material from burrow was collected by Dr.S.Gubin (Soil Cryology Lab, Pushchino, Russia) in august 2002.

Phylogenomics to define *Panagrolaimus n. sp* sp. nov.

To place the species in the genus *Panagrolaimus*, we conducted a broader multi-gene phylogenomic analysis using Maximum likelihood methods. Our analysis of a concatenated, partitioned alignment of 60 genes, and a coalescence-based approach using a broader set of 12,295 gene trees, retrieves the novel species as sister to all other sequenced *Panagrolaimus* species, but as an ingroup to *Propanagrolaimus*[31] (Fig.3C; Fig. S3B-C). Thus, the phylogenetic placement provides strong evidence that this animal belongs to a novel species. Furthermore, there is substantial sequence divergence between this novel species, and *Panagrolaimus* sp. PS1159 and *Panagrolaimus* sp. ES5, estimated to be on average 2.06 and 2.11 amino acid substitutions per site in our concatenated alignment, respectively. The substantial divergence is in line with previous data on ages of *Panagrolaimus* nematodes[30], and more broadly seen in nematodes, which can be hyper-diverse[32,33]. Our data also contradicts the assumption that parthenogenesis is a monophyletic trait[30] in the *Panagrolaimus* genus (Fig.3C). Using the gene-tree reconciliation approach implemented in GRAMPA, we explored whether extra sets of proteins in parthenogenetic species whether a result of auto- or allopolyploidy. The most parsimonious result, with extra proteins being basal to the lineage containing both parthenogenetic and sexual species, suggests an allopolyploid origin for these extra gene copies

182 (Fig.S6). Based on the Kolyma River location where the animal was unearthed, we propose the
183 following taxonomic classification and species name:
184 Phylum Nematoda Potts, 1932
185 Class Chromadorea Inglis 1983
186 Suborder Tylenchina Thorne, 1949
187 Family Panagrolaimidae Thorne, 1937
188 *Panagrolaimus* sp. nov.
189
190 ***C. elegans* dauer larvae and *Panagrolaimus n. sp.* might utilize similar mechanisms to**
191 **enter and remain in cryptobiotic state for prolonged periods of time**
192 In the absence of established genetic methods in *Panagrolaimus n. sp.* we referred to
193 the model *C. elegans* as a comparator system to gain insights into possible pathways for long
194 term survival[3,4,24,25]. The high-quality genome of *Panagrolaimus n. sp.* allowed us to compare
195 its molecular toolkit for cryptobiosis with that of *C. elegans*. We used orthology clustering and
196 phylogenetics to investigate whether the genome of *Panagrolaimus n. sp.* contains genes
197 previously implicated in cryptobiosis in the *C. elegans* dauer larva. Our analysis showed that
198 the like other *Panagrolaimus* species[34,35], *Panagrolaimus n. sp.* genome also encodes orthologs
199 to a *C. elegans* trehalose phosphate synthase gene (*tps-2*) and to a trehalose phosphatase gene
200 (*gob-1*) (Fig. 3D, supplementary file Orthology analysis). Furthermore, we found orthologs to
201 all *C. elegans* enzymes required for polyamine biosynthesis, the TCA cycle, glycolysis,
202 gluconeogenesis, and glyoxylate shunt (Fig.3D, supplementary file Orthology analysis)
203 suggesting that *Panagrolaimus n. sp.* might utilize a similar molecular tool kit as *C. elegans* to
204 facilitate survival of unfavorable conditions. Our earlier findings established that among
205 several developmental stages of *C. elegans*, only the dauer larva, formed during unfavorable
206 conditions (such as low nutrients and high population density) and in hypometabolic state could
207 survive anhydrobiosis and exposure to freezing[4,24]. To survive extreme desiccation, *C. elegans*
208 dauer larvae (in its hypometabolic state) need to be first preconditioned at high relative
209 humidity (98% RH) for 4 days[24]. During preconditioning, dauer larvae upregulate trehalose
210 biosynthesis that ensures their survival to harsh desiccation[24,25]. We tested whether
211 preconditioning also facilitates survival of *Panagrolaimus n. sp.*. As there is no dauer stage in
212 *Panagrolaimus* life cycle we performed our experiments with mixed populations of larval
213 stages. Although a small proportion of *Panagrolaimus n. sp.* individuals survive harsh
214 desiccation and freezing without preconditioning (Fig.4A), mixed populations of

215 *Panagrolaimus n. sp.* survive significantly (p value< 0.0001) in a higher proportion to harsh
216 desiccation upon preconditioning (Fig.4A). Similarly, preconditioning and desiccation further
217 enhanced survival rate of *Panagrolaimus n. sp.* to freezing (-80°C) (Fig.4A). Like *C. elegans*
218 dauer larva, *Panagrolaimus n. sp.* upregulate trehalose levels up to 20-fold upon
219 preconditioning (Fig.4B). We previously reported that, to upregulate trehalose levels upon
220 preconditioning, *C. elegans* dauer larva dissipate their fat reserves (Triacylglycerols) by
221 activating the glyoxylate shunt and gluconeogenic pathway[25]. Upon preconditioning, we found
222 that triacylglyceride (TAG) levels are significantly decreased in *Panagrolaimus n. sp.*
223 (Fig.S5A&B). To further investigate whether the acetyl-CoA derived from degradation of
224 TAGs culminate in trehalose, we applied the previously developed method of metabolic
225 labelling with ^{14}C-acetate in combination with 2D-TLC [4,25]. The ^{14}C-acetate metabolized by
226 the worms is incorporated into TAGs. Upon degradation of TAGs, ^{14}C-acetyl CoA is released
227 which acts as a precursor for trehalose biosynthesis. As shown in Fig. 4C, preconditioning led
228 to huge increase of radioactivity in trehalose and to smaller extent in some amino acids
229 (glycine/serine, phenylalanine; panels c and d). Interestingly, *Panagrolaimus n. sp.* displayed
230 an additional spot (Fig. 4D, enumerated as 7), that was not found in *C. elegans*. We identified
231 this spot as trehalose-6-phosphate (Fig.S5C-H), a precursor of trehalose, based on the
232 fragmentation pattern of the molecule, using mass spectrometry. Thus, to resist harsh
233 desiccation, like *C. elegans* dauer larvae, *Panagrolaimus n. sp.* might utilize the glyoxylate
234 shunt and consequently acetate derived from TAGs to synthesize trehalose. Detection of the
235 immediate precursor (trehalose-6-phosphate) suggests that the flux of metabolites is intense in
236 *Panagrolaimus n. sp*. Finally, we investigated whether *C. elegans* dauer larvae can also survive
237 in prolonged cryptobiotic state. Despite of preconditioning, the survival ability of desiccated
238 dauer larvae at room temperature declines very rapidly, with most larvae dead after around 10
239 days (Fig. 4E) (Fig. S4A&B). Direct freezing without any cryoprotectants at -80℃ leads to
240 almost instant death of the animals. To test whether combining these conditions could extend
241 the viability of dauer larvae (Fig. S4A&B), we transferred the desiccated larvae to -80℃.
242 Remarkably, under these conditions, there was no significant decline in viability even after 480
243 days (Fig. 4E). Moreover, after thawing, the animals resumed reproductive growth and
244 produced progeny in numbers like those of animals kept under control conditions (Fig. 4F).
245 Since we did not observe any reduction in the survival at any time points, this suggests that the
246 combination of anhydrobiosis and freezing can prolong the survival ability of dauer larvae.

Thus, *C. elegans* dauer larvae, when exposed to combination of cryptobiotic states can survive for extremely long periods of time.

Discussion

Our findings here indicate that some nematodes could survive in suspended animation for millenia. Along with the adaptive mechanisms of an organism, a naturally preserving ecosystem would synergistically aid the survival for prolonged periods. The Siberian permafrost is a unique repository for preserving organisms in sub-zero temperatures for millions of years. Expeditions in the past decade revived several organisms across various taxa from the Siberian permafrost[5,36,37,38]. The possibility to exploit permafrost as a source for reanimating multicellular animals was recognized already in 1936. A viable Cladocera crustacean *Chydorus sphaericus* preserved in the Transbaikalian permafrost for several thousand years[39,40] was discovered by P.N. Kapterev, who worked at the scientific station Skovorodino as a GULAG prisoner. Unfortunately, this extraordinary observation remained unnoticed for many decades.

The new nematode species from permafrost can now be placed into the genus *Panagrolaimus*[41], which contains several described parthenogenetic and gonochoristic species[30,42]. Many *Panagrolaimus* display adaptation to survival in harsh environments[21] and the genus includes the Antarctic species *P. davidi*[22]. The genus *Panagrolaimus* is exceptional in its morphological uniformity even among nematode species that are hard to classify based on morphology in general. Thus, species designation via microscopic (including SEM) analysis is unreliable, which is further complicated by the absence of males in parthenogenetic species. Males have important diagnostic features as spicules and pericloacal papillae, females differ from one species to another mainly by morphometrics, whereby the interspecies differences (absolute measures and ratios) may be very fine. Our specimens are close by absolute sizes and ratios to females of the bisexual species *Panagrolaimus detritophagus*[43]. The only non-overlapping morphometric character is index “b” (body length: pharynx length): 5.6–6.8 in *Panagrolaimus n. sp.* versus 4.4-5.1 in *P. detritophagus*.

Consequently, we turned to phylogenomics methods to place the species on the tree. This showed that this species is an outgroup to other known *Panagrolaimus* species, raising the possibility of a second independent evolution of parthenogenesis in the genus, in contrast to previous findings[42,31,30]. This will need to be confirmed through further sampling and genome sequencing of *Panagrolaimus* species. We found *Panagrolaimus n. sp.* to be triploid and thus a hybrid origin is possible, as seen in other parthenogenetic *Pangrolaimus*[30]. The

280 highly contiguous genome of *Panagrolaimus n. sp.* will allow for analyses of this trait in
281 comparison to other *Panagrolaimus* species currently being genome sequenced.

282 Our results provide a deeper insight into the homology of molecular and biochemical
283 mechanisms between *C. elegans* and *P. kolymaensis*, which are not only taxonomically but
284 also ecologically distinct. *C. elegans* can mostly be found in rotting fruits and plants in
285 temperate regions[44,45], while *Panagrolaimus* species are globally distributed and prevalent in
286 leaf litter and soil[42], including in harsh environments[21]. We show through orthology analysis
287 that the well-studied molecular pathways used by *C. elegans* larvae to enter the dauer state,
288 such as insulin[46,47] (DAF-11, DAF-2 & DAF-16), TGF-β[48] (DAF-7), steroid[49] (DAF-9, DAF-
289 12) are present in the genome of the *Panagrolaimus n. sp.* (Fig.S4C). While further functional
290 analyses are needed to study molecular pathways in detail, our results hint at convergence or
291 parallelism in the molecular mechanisms organizing dauer formation and cryptobiosis.

292 As mentioned earlier preconditioning enhances the survival of *Panagrolaimus n. sp*.
293 renders them desiccation tolerant. We previously reported that preconditioning elevates
294 trehalose biosynthesis in *C. elegans* dauer larvae and the elevated trehalose renders desiccation
295 tolerance by protecting the cellular membranes[24]. It is not surprising that *Panagrolaimus n. sp.*
296 upregulates trehalose, however the magnitude of trehalose elevation is higher than *C. elegans*
297 dauer larvae. This indicates that central regulators (DAF-16, DAF-12) of trehalose
298 upregulation may differentially regulate *tps-2* in *Panagrolaimus n. sp*[50,51,34]. Although
299 *Panagrolaimus n. sp.* utilizes the glyoxylate shunt and gluconeogenesis to upregulate trehalose
300 levels, it is intriguing to observe that they accumulate substantial levels of trehalose-6-
301 phosphate. Further investigation of this observation using perturbation experiments will
302 provide insights into molecular mechanisms of metabolic regulation in *Panagrolaimus n. sp.*
303 upon preconditioning. Our findings for the first time demonstrate that *C. elegans* dauer larvae
304 possess an inherent ability to survive freezing for prolonged periods if they undergo
305 anhydrobiosis. It is tempting to speculate that undergoing anhydrobiosis might be a survival
306 strategy of *C. elegans* to survive the seasonal changes in nature.

307 In summary our findings indicate that by adapting to survive cryptobiotic state for
308 short time frames in environments like permafrost, some nematode species gained the potential
309 for individual worms to remain in the state for geological timeframes. This raises the question
310 whether there is an upper limit to the length of time an individual can remain in the cryptobiotic
311 state, potentially only limited by drastic changes to the environment such as strong fluctuations
312 in ambient temperature, natural radioactivity, or other abiotic factors. These findings have

implications for our understanding of evolutionary processes since generation times could be stretched from days to millennia and long- term survival of individuals of species can lead to the refoundation of otherwise extinct lineages. This is particularly interesting in the case of parthenogenetic species, as the one described here, as each individual can found a new population without the need for mate finding, i.e. evading the cost of sex. Finally, understanding the precise mechanisms of long-term cryptobiosis and cues that lead to successful revivals can inform new methods for long term storage of cells and tissues.

320 **Methods**

321 **Materials and *C. elegans* strains**

322 [1-14C] -acetate (sodium salt) was purchased from Hartmann Analytic (Braunschweig,
323 Germany). All other chemicals were purchased from Sigma-Aldrich (Taufkirchen, Germany).
324 The *Caenorhabditis* Genetic Centre (CGC) which is funded by NIH Office of Research
325 Infrastructure Programs (P40 OD010440) provided *daf-2(e1370)* and *E. coli NA22* strains.
326

327 **Genomic DNA isolation from *Panagrolaimus n. sp* nematodes**

328 *Panagrolaimus n. sp.* nematodes (isofemale strain Pn2-1) were grown on several plates of
329 NGM agar plated with *E. coli NA22* bacteria at 20°C. Worms were collected from the plates,
330 washed with water at least three to five times by centrifugation at 1000 g to remove any residual
331 bacteria and any debris. The worm pellet was dissolved in 5 volumes of worm lysis buffer
332 (0.1M Tris-HCl pH=8.5, 0.1M NaCl, 50mM EDTA pH=8.0) and distributed in 1.5 ml of
333 microcentrifuge tubes. These tubes are incubated at -80°C for 20 minutes. 100 µl of Proteinase
334 'K' (20 mg/ml) was added to each tube and they are incubated at 60°C overnight. 625 µl of
335 cold GTC buffer (4M Guanidinium Thiocynate, 25mM Sodium citrate, 0.5% (v\v) N-
336 lauroylsarcosine, 7%(v/v) Beta Mercaptoethanol) was added to the tube, incubated on ice 30
337 min, and mixed by inverting every 10 min. 1 volume of phenol–chloroform-isoamyl alcohol
338 (pH=8) was added to the lysate and mixed by inverting the tube 10-15 times. Tubes were
339 centrifuged for 5 min at 10,000 g at 4°C to separate the phases. The upper aqueous phase was
340 carefully collected into a fresh tube. One volume of fresh chloroform was added and mixed by
341 inverting the tubes for 10-15 times and centrifuged for 5 min at 10,000 g at 4°C to separate the
342 phases. One volume of cold 5 M NaCl was added, mixed by inverting the tubes and incubated
343 on ice for 15 min. After incubation these tubes were centrifuged for 15 min at 12,000–16,000
344 g at 4°C. The supernatant containing the nucleic acids were slowly transferred into a fresh tube.
345 One volume of isopropanol was added to the tube, inverted few times, and incubated on ice for
346 30 minutes. After incubation, the tubes were centrifuged at 3000 g for 30–45 min at 25°C and
347 the supernatant was discarded without disturbing the pellet. The pellet was washed twice with
348 1 ml of 70% ethanol, tubes were centrifuged at 3000 g for 5 min and supernatant was discarded
349 and incubated at 37°C for 10-15 min to dry the pellet. The pellet was resuspended carefully in
350 TE buffer. The quality of the genomic DNA was analyzed with pulse field gel electrophoresis.
351
352

353 **Genome sequencing and assembly**

354 Long insert library has been prepared as recommended by Pacific Bioscienes according to
355 theprotocol 'Procedure & Checklist-Preparing gDNA Libraries Using the SMRTbell® Express
356 Template Preparation Kit 2.0'. In summary, RNAse treated HMW gDNA has been sheared to
357 20 kb fragments on the MegaRuptor™ device (Diagenode) and 10 µg sheared gDNA have
358 been used for library preparation. The PacBio SMRTbell™ library was size selected in two
359 fractions (9-13kb, > 13kb) using the BluePippin™ device with cassette definition of 0.75% DF
360 MarkerS1 3-10 kb Improved Recovery. The second fraction of the size selected library has
361 been loaded with 95 *p*M on plate on a Sequel SMRT cell (8M). Sequel polymerase 2.0 has
362 been used in combination with the v2 PacBio sequencing primer and the Sequel sequencing kit
363 2.0EA, runtime was 30 hours. We created PacBio CCS reads from the subreads .bam file using
364 PacBio's ccs command linetool (version4.2.0). We obtained 8.5Gb hiqh quality CCS reads
365 (HiFi reads) with a N50 of 14.4 kb. We ran HiCanu (version 2.2)[39] to create the contig
366 assembly. Blobtools[53] (version 1.1.1) was used to identify and remove bacterial contigs. The
367 final triploid contig assembly consists of 856 contigs has a N50 of 3.82 Mb and a size of
368 266Mb. The mitochondrial genome was created with the mitoHifi pipeline (version
369 2, https://github.com/marcelauliano/MitoHiFi) based on the assembled contigs and the closely
370 related reference mitochondrial genome of *Panagrellus redivivus* (strain: PS2298/MT8872,
371 ENAaccession: AP017464). The mitoHifi pipeline identified 49 mitochondrial contigs ranging
372 from 13-32Kb. The final annotated circular mitochondrial genome has a length of 17467 bp.
373 To identify pseudohaplotypes in the the *Panagrolaimus n. sp.* genome assembly, we selected
374 the longest isoform of each predicted protein-coding gene in our assembly and in the *C. elegans*
375 genome (downloaded from WormBase Parasite, release WBPS15) using AGAT (version 0.4.0)
376 and clustered them into orthologous groups (OGs) using OrthoFinder (version 2.5.2). We
377 identified OGs that contained three *Panagrolaimus* sequences (i.e. groups that were present as
378 single-copy in all three pseudohaplotypes) and used these to identify trios of multi-megabase
379 size contigs derived from the three pseudohaplotypes. We visualized synteny between the three
380 pseudohaplotypes using Circos to plot the positions of each homeolog (version 0.69-8).

381

382 **Genome annotation**

383 We used RepeatModeler 1.0.8 (http://www.repeatmasker.org/) with parameter '-engine ncbi'
384 to create a library of repeat families. This library was used with RepeatMasker 4.0.9 to

385 soft-mask the *Panagrolaimus* genome. To annotate genes, we cross mapped protein models
386 from an existing *Panagrolaimus* as external evidence in the Augustus based pipeline. We
387 evaluated the completeness of our predictions using BUSCO on the gVolante web interface.
388
389 **Orthology analysis**
390 We conducted a gene orthology analysis using genomic data from *Panagrolaimus n. sp*, the
391 Plectid nematode species from the permafrost, as well as genomic data from WormBase
392 Parasite (https://parasite.wormbase.org; accessed 17/12/2020): *Caenorhabditis elegans*,
393 *Diploscapter coronatus*, *Diploscapter pachys*, *Halicephalobus mephisto*, *Panagrellus*
394 *redivivus*, *Panagrolaimus davidi*, *Panagrolaimus* sp. ES5, *Panagrolaimus* sp. PS1159,
395 *Panagrolaimus superbus*, *Plectus sambesii*, and *Propanagrolaimus* sp. JU765. For plectids,
396 genomic resources are scarce. We therefore added transcriptome data of *Plectus murrayi*,
397 *Anaplectus granulosus*, *Neocamacolaimus parasiticus*, and *Stephanolaimus elegans*. The latter
398 three transcriptomes were kindly provided by Dr. Oleksandr Holovachov (Swedish museum of
399 natural history). The *Anaplectus granulosus*, and *Neocamacolaimus parasiticus* transcriptomes
400 have been published [55,56]. All three transcriptomes were assembled de novo with Trinity[57]. The
401 exact procedures are described in the respective publications[55,56] . The *Stephanolaimus elegans*
402 transcriptome was assembled in the same way as described for *Neocamacolaimus parasiticus*.
403 The *Plectus murrayi* transcriptome was built from raw reads deposited at NCBI (https://sra-
404 downloadb.be-md.ncbi.nlm.nih.gov/sos2/sra-pub-run-13/SRR6827978/SRR6827978.1;
405 accessed 22.12.2020). The transcriptome was assembled using Galaxy Trinity version 2.9.1[58],
406 [57] using all default options and including in silico normalization of reads before assembly.
407 Transdecoder (conda version 5.5.0)[59] was used to translate to amino acid sequence. Identical
408 reads were removed with cd-hit version 4.8.1[60,61], and the Trinity
409 get_longest_isoform_seq_per_trinity_gene.pl command[59] (Trinity conda version 2.8.5)
410 (Anaconda Software Distribution, Conda, Version 4.9.2, Anaconda, Nov. 2020); was used, to
411 remove shorter isoforms. Amino acid translated longest isoforms from genomic data were
412 extracted with AGAT (Dainat, https://www.doi.org/10.5281/zenodo.3552717) from genome
413 assembly FASTA files and genome annotation GFF3 files, using the
414 agat_convert_sp_gxf2gxf.pl command to convert all GFF3 files to the required GFF3 format,
415 and the agat_sp_keep_longest_isoform.pl as well as the agat_sp_extract_sequences.pl
416 commands to extract amino acid translated FASTA files. The headers and names of all FASTA
417 files were modified to allow for simple species assignment of each sequence in subsequent

418 analysis. The orthology analysis was conducted with OrthoFinder v. 2.5.1[62,63] using default
419 settings. For genes of interest, we constructed alignments with MAFFT v. 7.475[64] using the
420 localpair and maxiterate (1000) functions. We removed spurious sequences and areas that were
421 not well aligned with Trimal v. 1.4.rev22[65] (procedure stated in supplementary file Orthology
422 analysis below each phylogeny). We then ran phylogenetic analysis with Iqtree2 v. 2.0.6[66],
423 with -bb 1000 option, testing the model for each analysis (models eventually used stated in
424 supplementary file Orthology analysis). We also checked for PFAM domains using
425 Interproscan v. 5.50-84.0[67]. Part of the analysis was performed on the HPC RRZK CHEOPS
426 of the Regional Computing Centre (RRZK) of the University of Cologne. The phylogenies
427 were visualized with Dendroscope 3.7.6[68] and figures were created with Inkscape
428 (https://inkscape.org).
429
430 **Phylogenomics**
431 Sequences of 18S and 28S genes from 44 taxa across the *Propanagrolaimus*, *Panagrolaimus*,
432 *Panagrellus* and *Halicephalobus* genera (all listed in Supplementary information) were aligned
433 (MAFFT L-INS-I v7.475)[64], concatenated [69]and used to infer a species tree using maximum
434 likelihood via (IQTREE)[70] and partitioned by best-fit models of sequence evolution for both[71].
435 Nodal support was determined using 1000 bootstrap pseudoreplicates. A further 60 genes from
436 101 taxa (all listed in Supplementary information) were used to confirm the taxonomic
437 position using the supermatrix concatenation methods outlined above. Given the limitations of
438 differential gene sampling, we expanded our phylogenomic analyses to include a coalescence
439 approach using 12,295 ML gene trees inferred for orthogroups containing the target animal.
440 Instances of multiple genes per species per group were treated as paralogs/orthologs and
441 analysed using ASTRAL-Pro[72]. Given the number of copies of genes per orthogroup, we
442 explored whether auto or alloploidy was the source of extra genes observed using the gene-tree
443 reconciliation approach implemented in GRAMPA[75]. All gene trees rooted at the midpoint and
444 the final ASTRAL-pro species tree were used as inputs, with the most parsimonious result
445 analyzed further.
446
447 **Desiccation survival assay**
448 *C. elegans* dauer larvae desiccation assays were performed as described in[24]. *Panagrolaimus*
449 *n. sp* desiccation assays were performed similarly as described in[24] with mixed population
450 (Mixture of all larval stages and adults) of the nematodes.

451 **Exposure of nematodes to extreme environments**

452 *C. elegans* dauer larvae or mixed population (Mixture of all larval stages and adults) of
453 *Panagrolaimus n. sp* nematodes were preconditioned and desiccated as described in[24], then
454 transferred to elevated temperature of 34°C, freezing (-80°C) and anoxia. Anoxic environment
455 was generated in a desiccation chamber at 60%RH by flushing the Nitrogen gas into the
456 chamber. The concentration of oxygen inside the chamber was monitored. After each timepoint
457 they were rehydrated with 500 µl of water for 2-3 hours. Rehydrated worms were transferred
458 to NGM agar plates with *E. Coli NA22* as food. Survivors were counted after overnight
459 incubation at 15°C. Each experiment was performed on two different days with at least two
460 technical replicates.

461

462 **Trehalose quantification from nematode lysates**

463 Trehalose measurements were performed as described in previous reports[25].

464

465 **Radiolabeling, metabolite extraction and 2D-TLC**

466 The above-mentioned procedures were performed according to previous reports[3,25].

467 **Identification of trehalose-6-phosphate from TLC plates**

468 Normalised aqueous fractions from the non-preconditioned and preconditioned samples were
469 separated by high performance thin layer chromatography (HPTLC), using 1-propanol-
470 methanol-ammonia (32%)-water (28:8:7:7 v/v/v/v) as first, dried for 15 min and 1-butanol-
471 acetone-glacial acetic acid–water (35:35:7:23 v/v/v/v) second dimension respectively. Using
472 the trehalose as a standard on both dimensions of the TLC, the regions of interest were scrapped
473 out from the TLCs. The scraped-out silica was extracted with 10 ml of 50% methanol twice.
474 The fractions were combined, dried under vacuum and dissolved in 100 µl of MS mix solution
475 containing 4:2:1 (Isopropanol:Methanol:Chloroform) with 7.5 mM ammonium formate. Mass
476 spectrometric analysis was performed on a Q Exactive instrument (Thermo Fischer Scientific,
477 Bremen, DE) equipped with a robotic nanoflow ion source TriVersa NanoMate (Advion
478 BioSciences, Ithaca, USA) using nanoelectrospray chips with a diameter of 4.1 µm. The ion
479 source was controlled by the Chipsoft 8.3.1 software (Advion BioSciences). Ionization voltage
480 was + 0.96 kV in negative mode; backpressure was set at 1.25 psi. The temperature of the ion
481 transfer capillary was 200°C; S-lens RF level was set to 50%. FT MS spectra were acquired
482 within the range of m/z 50–750 at the mass resolution of R m/z 200 = 140000; automated gain
483 control (AGC) of 3×10^6 and with the maximal injection time of 3000 ms. FT MS/MS spectra

484 were acquired within the range of m/z 50–750 at the mass resolution of R m/z 200 = 140000;
485 automated gain control (AGC) of 3×10^4 and with a maximal injection time of 30 s.
486
487 **Triacylglycerols measurement from *Panagrolaimus n. sp* lysates**
488 Non-preconditioned and preconditioned pellets were lysed in 200 µl of isopropanol with 0.5
489 mm Zircornium beads twice for 15 min. The lysates were centrifuged at 1300 g for 5 min. The
490 supernatant was carefully collected without any debris, 20 µl of the lysate was used for protein
491 estimation. Normalization was performed according to soluble protein levels, supernatant
492 volumes corresponding to 50-100 µg of proteins were dried in the desiccator. 700 µl of IS
493 ((10:3 (Methyl tert-butyl ether: ethanol)) mix (warmed to room temperature) was added to
494 dried samples and left on the shaker for 1 hour. The samples were centrifuged at 1400 rpm and
495 4°C. 140 µl of water was added and left on the shaker for 15 min. These samples were
496 centrifuged at 13400 rpm for 15 min. The upper organic fraction was collected and transferred
497 to 1.5 ml glass vial and left for drying in the desiccator. The dried samples were reconstituted
498 in a volume of 300 µl of 4:2:1 (Isopropanol:Methanol:Chloroform). Volume corresponding to
499 1 µg was used for injection.
500 LC-MS/MS analysis was performed on a high-performance liquid chromatography
501 system (Agilent 1200 HPLC) coupled to a Xevo G2-S QTof (Waters). The samples were
502 resolved on a reverse phase C18 column (Cortecs C18 2.7um from Waters) with
503 50:50:0.1:1% (Water:Methanol:Formicacid:1MAmmoniumformate) and 25:85:0.1:1%
504 (Acetonitrile:Isopropanol:Formic acid:1M Ammonium formate) as mobile phase. The
505 following gradient program was used: Eluent B from 0 % to 100 % within 12 min; 100 % from
506 12 min to 17min; 0 % from 17 min to 25 min. The flow rate was set at 0.3 ml/min. The samples
507 were normalised according to the total protein concentration and the worm numbers. TAG
508 50:00:00 was used as internal standard. Skylinesoftware
509 (https://skyline.ms/project/home/software/Skyline/begin.view) was used to analyse the raw
510 data. TAGs were extracted from Lipidmaps (https://www.lipidmaps.org/) database.
511
512
513
514
515
516

517 **Author contributions**

518 AS, VG, PS, TK conceived and designed the study. AS, VG, TH, MP, AT, GH, MH, ER, PS
519 and TK contributed to the original draft. AS performed cultivation of nematode, provided
520 samples for scanning electron microscopy and radiocarbon dating. VG performed desiccation
521 survival assays, trehalose measurement, 2D-TLC of metabolites, trehalose-6-phosphate
522 detection, combination of cryptobiosis experiments, genomic DNA isolation from
523 *Panagrolaimus n. sp.*, assembled the data from all the authors, prepared the figures and revised
524 the manuscript. MP performed genome assembly. TH conducted orthology analyses and single
525 gene phylogenies and contributed to figures. AT provided morphological description, light, and
526 scanning electron microscopy. LS analyzed the genome assembly and created figures. GMH
527 performed the phylogenetic, MUL analyses. ST performed triacylglycerols measurements,
528 trehalose-6-phosphate detection with suggestions from Andrej Shevchenko. MH annotated
529 supplementary table 3. PS performed genome annotation and supervised TH and LS. EWM
530 supervised MP and had overall responsibility for sequencing and assembly including funding
531 it.
532
533
534
535
536
537
538
539
540
541
542
543
544
545
546
547
548
549

Acknowledgements

VG is thankful to Andrej Shevchenko, members of Kurzchalia lab for helpful discussions and the core facilities of MPI-CBG for assistance. We are grateful to Dr. S. Gubin for field study and sampling, our colleagues in Soil Cryology Lab, Pushchino and North-East Scientific Station in Chersky, Republic of Sakha (Yakutia) for their help and cooperation. The authors thank Long Read Team of the DRESDEN-concept Genome Center, DFG NGS Competence Center, part of the Center for Molecular and Cellular Bioengineering (CMCB), Technische Universität Dresden and MPI-CBG. GMH is funded by a UCD Ad Astra Fellowship. This work was supported by the Russian Foundation for Basic Research (19-29-05003-mk) to AS and ER. VG and TK acknowledge the financial support from the Volkswagen Foundation (Life? research grant 92847). PS and TH are supported by a DFG ENP grant to PS (DFG project 434028868). The authors are thankful to Richard Roy and Jens Bast for critical reading the manuscript. We thank Iain Pattern for suggestions in writing the manuscript. The funders have no role in the design of the study.

Conflict of interest:

The authors declare they have no conflict of interest relating to the content of this article.

References

1. Hibshman, J. D., Clegg, J. S. & Goldstein, B. Mechanisms of Desiccation Tolerance: Themes and Variations in Brine Shrimp, Roundworms, and Tardigrades. *Front. Physiol.* **11**, 592016 (2020).
2. Erkut, C. *et al.* Molecular Strategies of the Caenorhabditis elegans Dauer Larva to Survive Extreme Desiccation. *PLoS ONE* **8**, e82473 (2013).
3. Gade, V. R., Traikov, S., Oertel, J., Fahmy, K. & Kurzchalia, T. V. C. elegans possess a general program to enter cryptobiosis that allows dauer larvae to survive different kinds of abiotic stress. *Sci. Rep.* **10**, 13466 (2020).
4. Shatilovich, A. V. *et al.* Viable Nematodes from Late Pleistocene Permafrost of the Kolyma River Lowland. *Dokl. Biol. Sci.* **480**, 100–102 (2018).
5. Shmakova, L. *et al.* A living bdelloid rotifer from 24,000-year-old Arctic permafrost. *Curr. Biol.* **31**, R712–R713 (2021).
6. Keilin, D. The Leeuwenhoek Lecture - The problem of anabiosis or latent life: history and current concept. *Proc. R. Soc. Lond. Ser. B - Biol. Sci.* **150**, 149–191 (1959).
7. Cano, R. & Borucki, M. Revival and identification of bacterial spores in 25- to 40-million-year-old Dominican amber. *Science* **268**, 1060–1064 (1995).
8. Shen-Miller, J. Sacred lotus, the long-living fruits of China Antique. *Seed Sci. Res.* **12**, 131–143 (2002).
9. Guidetti, R. & Jönsson, K. I. Long-term anhydrobiotic survival in semi-terrestrial micrometazoans. *J. Zool.* **257**, 181–187 (2002).
10. Tsujimoto, M., Imura, S. & Kanda, H. Recovery and reproduction of an Antarctic tardigrade retrieved from a moss sample frozen for over 30 years. *Cryobiology* **72**, 78–81 (2016).
11. Kagoshima, H. *et al.* Multi-decadal survival of an Antarctic nematode, Plectus murrayi, in a -20°C stored moss sample. *CryoLetters* **33**, 280–288 (2012).
12. Steiner, G. & Florence E, A. Resuscitation of the nematode Tylenchus polyhypnus, n. sp., after almost 39 years' dormancy. *J. Wash. Acad. Sci.* **36**, 97–99.
13. Gilichinsky, D. A. *et al.* Microbial Populations in Antarctic Permafrost: Biodiversity, State, Age, and Implication for Astrobiology. *Astrobiology* **7**, 275–311 (2007).
14. Rivkina, E. *et al.* Earth's perennially frozen environments as a model of cryogenic planet ecosystems. *Permafr. Periglac. Process.* **29**, 246–256 (2018).

15. Sipes, K. *et al.* Eight Metagenome-Assembled Genomes Provide Evidence for Microbial Adaptation in 20,000- to 1,000,000-Year-Old Siberian Permafrost. *Appl. Environ. Microbiol.* **87**, (2021).
16. Liang, R. *et al.* Genomic reconstruction of fossil and living microorganisms in ancient Siberian permafrost. *Microbiome* **9**, 110 (2021).
17. Gilichinsky, D. A. & Rivkina, E. M. Permafrost Microbiology. 7 (2011).
18. Yashina, S. *et al.* Regeneration of whole fertile plants from 30,000-y-old fruit tissue buried in Siberian permafrost. *Proc. Natl. Acad. Sci.* **109**, 4008–4013 (2012).
19. Adhikari, B. N., Wall, D. H. & Adams, B. J. Desiccation survival in an Antarctic nematode: molecular analysis using expressed sequenced tags. *BMC Genomics* **10**, 69 (2009).
20. Tyson, T. *et al.* A molecular analysis of desiccation tolerance mechanisms in the anhydrobiotic nematode Panagrolaimus superbus using expressed sequenced tags. *BMC Res. Notes* **5**, 68 (2012).
21. McGill, L. M. *et al.* Anhydrobiosis and Freezing-Tolerance: Adaptations That Facilitate the Establishment of Panagrolaimus Nematodes in Polar Habitats. *PLOS ONE* **10**, e0116084 (2015).
22. Thorne, M. A. S., Kagoshima, H., Clark, M. S., Marshall, C. J. & Wharton, D. A. Molecular Analysis of the Cold Tolerant Antarctic Nematode, Panagrolaimus davidi. *PLoS ONE* **9**, e104526 (2014).
23. Sandhove, J., Spann, N. & Ristau, K. The Anhydrobiotic Potential of the Terrestrial Nematodes *Plectus parietinus* and *Plectus velox*: Anhydrobiosis OF *Plectus parietinus* and *P. velox*. *J. Exp. Zool. Part Ecol. Genet. Physiol.* **325**, 434–440 (2016).
24. Erkut, C. *et al.* Trehalose Renders the Dauer Larva of Caenorhabditis elegans Resistant to Extreme Desiccation. *Curr. Biol.* **21**, 1331–1336 (2011).
25. Erkut, C., Gade, V. R., Laxman, S. & Kurzchalia, T. V. The glyoxylate shunt is essential for desiccation tolerance in C. elegans and budding yeast. *elife* **5**, (2016).
26. Zanina, O. G., Gubin, S. V., Kuzmina, S. A., Maximovich, S. V. & Lopatina, D. A. Late-Pleistocene (MIS 3-2) palaeoenvironments as recorded by sediments, palaeosols, and ground-squirrel nests at Duvanny Yar, Kolyma lowland, northeast Siberia. *Quat. Sci. Rev.* **30**, 2107–2123 (2011).
27. Murton, J. B. *et al.* Palaeoenvironmental Interpretation of Yedoma Silt (Ice Complex) Deposition as Cold-Climate Loess, Duvanny Yar, Northeast Siberia: Palaeoenvironmental

687 Interpretation of Yedoma Silt, Duvanny Yar. *Permafr. Periglac. Process.* **26**, 208–288
688 (2015).
689 28.Abramov, A., Vishnivetskaya, T. & Rivkina, E. Are permafrost microorganisms as old as
690 permafrost? *FEMS Microbiol. Ecol.* **97**, fiaa260 (2021).
691 29.Gilichinsky, D. A., Wagener, S. & Vishnevetskaya, T. A. Permafrost microbiology.
692 *Permafr. Periglac. Process.* **6**, 281–291 (1995).
693 30.Schiffer, P. H. *et al.* Signatures of the Evolution of Parthenogenesis and Cryptobiosis in the
694 Genomes of Panagrolaimid Nematodes. *iScience* **21**, 587–602 (2019).
695 31.Schiffer, P. H. *et al.* Developmental variations among Panagrolaimid nematodes indicate
696 developmental system drift within a small taxonomic unit. *Dev. Genes Evol.* **224**, 183–188
697 (2014).
698 32.Dey, A., Chan, C. K. W., Thomas, C. G. & Cutter, A. D. Molecular hyperdiversity defines
699 populations of the nematode Caenorhabditis brenneri. *Proc. Natl. Acad. Sci.* **110**, 11056–
700 11060 (2013).
701 33.Cutter, A. D. Divergence Times in Caenorhabditis and Drosophila Inferred from Direct
702 Estimates of the Neutral Mutation Rate. *Mol. Biol. Evol.* **25**, 778–786 (2008).
703 34.Seybold, A. C., Wharton, D. A., Thorne, M. A. S. & Marshall, C. J. Investigating trehalose
704 synthesis genes after cold acclimation in the Antarctic nematode *Panagrolaimus* sp. DAW1.
705 *Biol. Open* bio.023341 (2017) doi:10.1242/bio.023341.
706 35.Evangelista, C. C. S. *et al.* Multiple genes contribute to anhydrobiosis (tolerance to extreme
707 desiccation) in the nematode Panagrolaimus superbus. *Genet. Mol. Biol.* **40**, 790–802
708 (2017).
709 36.Malavin, S., Shmakova, L., Claverie, J.-M. & Rivkina, E. Frozen Zoo: a collection of
710 permafrost samples containing viable protists and their viruses. *Biodivers. Data J.* **8**, e51586
711 (2020).
712 37.Krivushin, K. *et al.* Two Metagenomes from Late Pleistocene Northeast Siberian
713 Permafrost. *Genome Announc.* **3**, e01380-14 (2015).
714 38.Zhou, J. *et al.* Phylogenetic diversity of a bacterial community determined from Siberian
715 tundra soil DNA. *Microbiology* **143**, 3913–3919 (1997).
716 39.Kapterev, P. Anabiosis in the conditions of permanent congelation. *Izv Akad Nauk SSSR Ser*
717 *Biol* **6**, 1073–1088 (1936).
718 40.Kapterev, P. New data on revitalization of organisms from perpetually frozen grounds. *CR*
719 *Acad Sci URSS* **20**, 315–317 (1938).

720 41.Andrássy, I. *Klasse Nematoda*. (Gustav Fischer Verlag, 1984).
721 42.Lewis, S. C. *et al.* Molecular evolution in Panagrolaimus nematodes: origins of
722 parthenogenesis, hermaphroditism and the Antarctic species P. davidi. *BMC Evol. Biol.* **9**,
723 15 (2009).
724 43.Andrássy, I. *Free-living Nematodes of Hungary*. (Hungarian Natural History Museum,
725 2005).
726 44.Schulenburg, H. & Félix, M.-A. The Natural Biotic Environment of *Caenorhabditis*
727 *elegans*. *Genetics* **206**, 55–86 (2017).
728 45.Frézal, L. & Félix, M.-A. C. elegans outside the Petri dish. *eLife* **4**, e05849 (2015).
729 46.Gems, D. *et al.* Two pleiotropic classes of daf-2 mutation affect larval arrest, adult behavior,
730 reproduction, and longevity in Caenorhabditis elegans. *Genetics* **150**, 129–155 (1998).
731 47.Vowels, J. J. & Thomas, J. H. Multiple chemosensory defects in daf-11 and daf-21 mutants
732 of Caenorhabditis elegans. *Genetics* **138**, 303–316 (1994).
733 48.Ren Peifeng *et al.* Control of C. elegans Larval Development by Neuronal Expression of a
734 TGF-β Homolog. *Science* **274**, 1389–1391 (1996).
735 49.Gerisch, B., Weitzel, C., Kober-Eisermann, C., Rottiers, V. & Antebi, A. A Hormonal
736 Signaling Pathway Influencing C. elegans Metabolism, Reproductive Development, and
737 Life Span. *Dev. Cell* **1**, 841–851 (2001).
738 50.Penkov, S. *et al.* Integration of carbohydrate metabolism and redox state controls dauer
739 larva formation in Caenorhabditis elegans. *Nat. Commun.* **6**, 8060 (2015).
740 51.Penkov, S. *et al.* A metabolic switch regulates the transition between growth and diapause
741 in C. elegans. *BMC Biol.* **18**, 31 (2020).
742 52.Nurk, S. *et al.* HiCanu: accurate assembly of segmental duplications, satellites, and allelic
743 variants from high-fidelity long reads. *Genome Res.* **30**, 1291–1305 (2020).
744 53.Laetsch, D. R. & Blaxter, M. L. BlobTools: Interrogation of genome assemblies.
745 *F1000Research* **6**, 1287 (2017).
746 54.Brůna, T., Hoff, K. J., Lomsadze, A., Stanke, M. & Borodovsky, M. BRAKER2: automatic
747 eukaryotic genome annotation with GeneMark-EP+ and AUGUSTUS supported by a
748 protein database. *NAR Genomics Bioinforma.* **3**, lqaa108 (2021).
749 55.Smythe, A. B., Holovachov, O. & Kocot, K. M. Improved phylogenomic sampling of free-
750 living nematodes enhances resolution of higher-level nematode phylogeny. *BMC Evol. Biol.*
751 **19**, 121 (2019).

752 56.Ahmed, M., Adedidran, F. & Holovachov, O. A draft transcriptome of a parasite
753 Neocamacolaimus parasiticus (Camacolaimidae, Plectida). *J. Nematol.* **53**, 1–4 (2021).
754 57.Grabherr, M. G. *et al.* Full-length transcriptome assembly from RNA-Seq data without a
755 reference genome. *Nat. Biotechnol.* **29**, 644–652 (2011).
756 58.Goecks, J., Nekrutenko, A., Taylor, J. & Galaxy Team, T. Galaxy: a comprehensive
757 approach for supporting accessible, reproducible, and transparent computational research in
758 the life sciences. *Genome Biol.* **11**, R86 (2010).
759 59.Haas, B. J. *et al.* De novo transcript sequence reconstruction from RNA-seq using the
760 Trinity platform for reference generation and analysis. *Nat. Protoc.* **8**, 1494–1512 (2013).
761 60.Li, W. & Godzik, A. Cd-hit: a fast program for clustering and comparing large sets of
762 protein or nucleotide sequences. *Bioinformatics* **22**, 1658–1659 (2006).
763 61.Fu, L., Niu, B., Zhu, Z., Wu, S. & Li, W. CD-HIT: accelerated for clustering the next-
764 generation sequencing data. *Bioinformatics* **28**, 3150–3152 (2012).
765 62.Emms, D. M. & Kelly, S. OrthoFinder: solving fundamental biases in whole genome
766 comparisons dramatically improves orthogroup inference accuracy. *Genome Biol.* **16**, 157
767 (2015).
768 63.Emms, D. M. & Kelly, S. OrthoFinder: phylogenetic orthology inference for comparative
769 genomics. *Genome Biol.* **20**, 238 (2019).
770 64.Katoh, K. & Standley, D. M. MAFFT Multiple Sequence Alignment Software Version 7:
771 Improvements in Performance and Usability. *Mol. Biol. Evol.* **30**, 772–780 (2013).
772 65.Capella-Gutierrez, S., Silla-Martinez, J. M. & Gabaldon, T. trimAl: a tool for automated
773 alignment trimming in large-scale phylogenetic analyses. *Bioinformatics* **25**, 1972–1973
774 (2009).
775 66.Minh, B. Q. *et al.* IQ-TREE 2: New Models and Efficient Methods for Phylogenetic
776 Inference in the Genomic Era. *Mol. Biol. Evol.* **37**, 1530–1534 (2020).
777 67.Jones, P. *et al.* InterProScan 5: genome-scale protein function classification. *Bioinformatics*
778 **30**, 1236–1240 (2014).
779 68.Huson, D. H. & Scornavacca, C. Dendroscope 3: An Interactive Tool for Rooted
780 Phylogenetic Trees and Networks. *Syst. Biol.* **61**, 1061–1067 (2012).
781 69.Kück, P. & Meusemann, K. FASconCAT: Convenient handling of data matrices. *Mol.*
782 *Phylogenet. Evol.* **56**, 1115–1118 (2010).

70. Nguyen, L.-T., Schmidt, H. A., von Haeseler, A. & Minh, B. Q. IQ-TREE: A Fast and Effective Stochastic Algorithm for Estimating Maximum-Likelihood Phylogenies. *Mol. Biol. Evol.* **32**, 268–274 (2015).
71. Kalyaanamoorthy, S., Minh, B. Q., Wong, T. K. F., von Haeseler, A. & Jermiin, L. S. ModelFinder: fast model selection for accurate phylogenetic estimates. *Nat. Methods* **14**, 587–589 (2017).
72. Zhang, C., Scornavacca, C., Molloy, E. K. & Mirarab, S. ASTRAL-Pro: Quartet-Based Species-Tree Inference despite Paralogy. *Mol. Biol. Evol.* **37**, 3292–3307 (2020).
73. Ranallo-Benavidez, T. R., Jaron, K. S. & Schatz, M. C. GenomeScope 2.0 and Smudgeplot for reference-free profiling of polyploid genomes. *Nat. Commun.* **11**, 1432 (2020).
74. Kokot, M., Długosz, M. & Deorowicz, S. KMC 3: counting and manipulating k-mer statistics. *Bioinformatics* **33**, 2759–2761 (2017).
75. Thomas, GWC., Ather, H. S., Hahn, W. Matthew. Gene-Tree Reconciliation with MUL-Trees to Resolve Polyploidy Events. Systematic Biology 66, 1007-1018 (2017).

Figure legends

Figure 1. Study site.

a) location of the Duvanny Yar outcrope on the Kolyma River, northeastern Siberia, Russia. b) view of the upper part of outcrop composed of ice wedges and permafrost silty deposits. c) lithostratigraphic scheme of deposits, showing location of studied rodent borrow (red circle). d) fossil rodent burrow with herbaceous litter and seeds buried in permafrost deposits; m a.r.l. = meters above river level.

Figure 2. General morphology of *Panagrolaimus n. sp*., female.

Scanning electron pictures (a, c), light microscopy photographs (e, f) and graphic presentations (b, d, g) of holotype: a, b) entire body, c, d) anterior ends, e) anterior body, f) perivulvar body region, g) tail. Abbreviations: l.f. – lateral field, ov – ovary, pro – procorpus of the pharynx, t.b. – terminal bulb of the pharynx, u – uterus with eggs, v – vulva, v.p. – ventral pore. Scale bars: a, d, e, f, g – 20 µm, b – 100 µm, c – 2 µm.

882 **Figure 3. Genome assembly and phylogenomics reveals that the newly discovered**
883 ***Panagrolaimus n. sp* species is triploid.**
884 a) Kmer spectra of the *Panagrolaimus n. sp* PacBio HiFi data. Kmers of length 19 were counted
885 using Jellyfish. b) Circos plot showing the triploid structure of the *Panagrolaimus n. sp*
886 genome. Lines represent the position of 6,715 homeologs in eight contigs that comprise 39.9
887 Mb (15%) of the assembly. Homeologs were identified by clustering protein-coding genes into
888 orthogroups using OrthoFinder and selecting groups containing three sequences. Contig IDs
889 and scale is shown. c) Inferred species tree for all taxa. The maximum likelihood tree inferred
890 using a concatenated supermatrix (18S and 28S genes) with bootstrap support values is
891 displayed. All genera are represented as monophyletic clades. *Panagrolaimus n. sp* is
892 highlighted in red and basal to all other *Panagrolaimus* taxa. Internal nodes, where all
893 subsequent branches represent identical sequences, are displayed with a black star. d)
894 *Panagrolaimus n. sp.* possesses *C. elegans* gene orthologs to enzymes required for TCA cycle,
895 glyoxylate shunt, glycolysis, gluconeogenesis, trehalose synthesis, and polyamine synthesis.
896 Black filled circles: Ortholog presence suggested by orthogroup clustering, phylogenetic
897 analysis, and domain architecture. White filled circles: No ortholog found via current analysis.
898 Coloured filled circles: Presence of *Panagrolaimus n. sp.* gene(s), related to several *C. elegans*
899 genes (all genes of same colour) that are all co-orthologous to that gene (those genes). Label:
900 *C. elegans* enzyme names and orthogroup that contains that gene according to our orthogroup
901 clustering.
902
903
904
905
906
907
908
909
910
911
912
913
914

Figure 4. *C. elegans* dauer larvae and *Panagrolaimus n. sp.* might utilize similar mechanisms to survive cryptobiosis.

a) Survival rate of *Panagrolaimus n. sp.* nematodes to desiccation and freezing (-80°C). Error bars indicate standard error of mean of two independent experiments with two technical replicates performed on two different days. Statistical comparison was performed using unpaired t test with Welch correction. n.s. $p > 0.05$, ****$p < 0.0001$. For desiccation (non-preconditioned) n = 289, freezing (non-preconditioned) n = 675, desiccation (preconditioned at 98%RH) n = 953 and freezing (preconditioned at 98%RH) n = 1295. b) *Panagrolaimus n. sp.* nematodes and *daf-2(e1370)* dauer larvae upregulate trehalose levels upon preconditioning at 98%RH. Error bars indicate standard error of mean of two independent experiments with three replicates performed on two different days. Statistical comparison was performed using two-way ANOVA with Holm-Sidak's multiple comparison test, ****$p < 0.0001$. c-d) 2D-thin layer chromatography of ^{14}C-acetate labelled metabolites from *Panagrolaimus n. sp.* that were non-preconditioned and preconditioned at 98%RH. Enumerated spots indicate trehalose (1), glucose (2), glutamate (3), glutamine (4), serine/glycine (5) and phenylalanine (6). Representative images from at least two independent experiments performed on two different days. e) Desiccated *daf-2 (e1370)* dauer larvae survive to freezing (-80°C) for an extremely long period. Error bars indicate standard error of mean of two independent experiments with two technical replicates performed on two different days. f) Brood size of desiccated dauer larvae exposed to freezing remain like that non- desiccated dauer larvae. Average brood size is the mean of seven dauer larvae per each condition. Statistical comparison was performed by using non-parametric Kolmogorov-smirnov test n.s $p>0.05$.

Figure S1. Calibration of a radiocarbon (^{14}C) date.

Radiocarbon date (44,315±405 BP) and calibrated age (45,839 -- 47,769 cal BP) of plant material collected from buried borrow P-1320. Radiocarbon ages were converted to calendar age equivalents with the OxCal V.4.4 program using the IntCal20 calibration curve. Pink-shaded area — radiocarbon date with standard deviation; grey-shaded area — radiocarbon date projection on the calibration curve with 95.4% probability.

Figure S2. Morphology of *Panagrolaimus n. sp* sp. n., female.

Graphic presentations of holotype (a,b) and SEM pictures (c-i): a) anterior body, b) female reproductive branch, c–e) anterior end of three different female specimens, f) anterior part of the lateral ridge, g) vulva, h) ventral excretory/secretory pore, i) posterior body with anus and lateral ridge. Scale bars: a,b - 50 µm, c,i - 3 µm, d - 2 µm, e –1 µm, f,h - 5 µm, g - 10 µm, .

1013 **Figure S3. Phylogenies inferred for genes sets using both concatenation and coalescence**
1014 **approaches.**
1015 a) The ploidy level was analysed with *Smudgeplot* v0.2.1[73]. KMC version 3.1.0[74] was used
1016 to count the 21-mers in the PacBio CCS reads. Then we ran *smudgeplot.py* to determine the
1017 lower and upper coverage cut-offs. These were determined to be 14 and 380. 21-mers with a
1018 coverage between 14 and 380 were filtered with kmc_tools. Then, we computed the k-mer
1019 pairs from the filtered 21-mers by running *smudgeplot.py hetkmers*. Finally, the produced a
1020 smudgeplot shows an estimated ploidy of 3. b) Species tree inferred for 12,295 gene trees using
1021 coalescence approach. The species tree implemented using the coalescence approach with
1022 orthogroup gene tree is displayed. Novel species in this study are displayed in red. All nodes
1023 have a posterior probability of 1. c) Species tree inferred for 102 taxa**.** The maximum likelihood
1024 tree inferred using a concatenated supermatrix of 60 genes is displayed. Bootstrap values are
1025 only displayed for nodes with less than 100% support. The platyhelminth *Macrostum lignano*
1026 serves as an outgroup for rooting. The ancestral *Panagrolaimus*, sister to all others within the
1027 *Panagrolaimus* genus, is highlighted in red.
1028
1029
1030
1031
1032
1033
1034
1035
1036
1037
1038
1039
1040
1041
1042
1043
1044

1045 **Figure S4. Combination of cryptobiotic states enhances survival of *C. elegans* dauer**
1046 **larvae.**
1047 a) Desiccated dauer larvae manifest enhanced survival rate to heat stress (34°C). Error bars
1048 indicate standard deviation of two independent experiments with two technical replicates. b)
1049 Desiccated dauer larvae display enhances survival rate to anoxia. Error bars indicate standard
1050 deviation of two independent experiments with two technical replicates. Statistical
1051 comparison was performed by paired two tailed t-test. *$p<0.05$. c) *Panagrolaimus n. sp.*
1052 possesses gene orthologs to most genes implicated in dauer formation and metabolism in *C.*
1053 *elegans*. Black filled circles: Ortholog presence suggested by orthogroup clustering,
1054 phylogenetic analysis, and domain architecture. White filled circles: No ortholog found via
1055 current analysis (in all cases these *C. elegans* genes did not cluster with any *Panagrolaimus*
1056 genes in the orthogroup clustering). Label: *C. elegans* enzyme names and orthogroup that
1057 contains that gene according to our orthogroup clustering.
1058
1059
1060
1061
1062
1063
1064
1065
1066
1067
1068
1069
1070
1071
1072
1073
1074
1075
1076
1077
1078

1079 **Figure S5. *Panagrolaimus n. sp.* reduces triacylglycerols (TAGs) levels and accumulates**
1080 **trehalose-6-phosphate upon preconditioning at 98%RH**.
1081 a) 1D-Thin layer chromatography of acetate labelled organic fractions of non-preconditioned
1082 (1) and preconditioned (2) *P. kolymaensis*. b) Mass spectrometric quantification of TAG levels
1083 of non-preconditioned (1) and preconditioned (2) *P. kolymaensis*. Error bars indicate standard
1084 deviation of two biological replicates with two technical replicates. Statistical analysis was
1085 performed using unpaired t-test with Welch correction **$p < 0.001$. c-d) non-preconditioned
1086 and preconditioned mass spectrum of an empty region, e-f) spot 1 (trehalose), g-h) spot 7
1087 (trehalose-6-phosphate) scraped out and extracted from the 2D-TLC.
1088
1089
1090
1091
1092
1093
1094
1095
1096
1097
1098
1099
1100
1101
1102
1103
1104
1105
1106
1107
1108
1109
1110
1111

1112 **Figure S6. Exploring a possible allopolyploid origin for extra proteins.**

1113 Gene-tree reconciliation was used to determine whether extra sets of proteins across
1114 orthogroups originate through auto- or allopolyploidy. Different copies of proteins (designated
1115 by '+' and '*') suggest an allopolyploid origin. Parthenogenetic species are highlighted in bold.

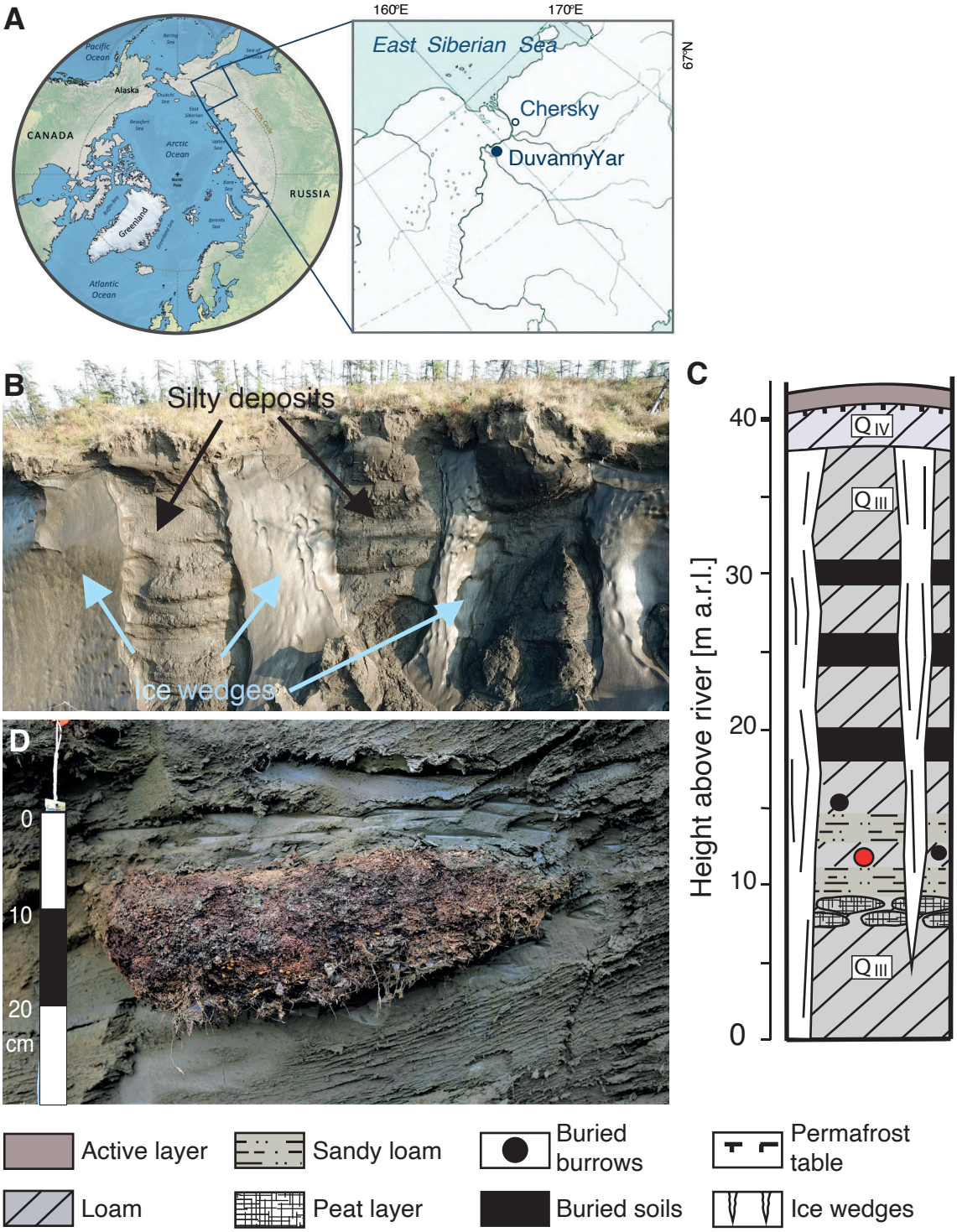

Figure 1
Shatilovich *et al*

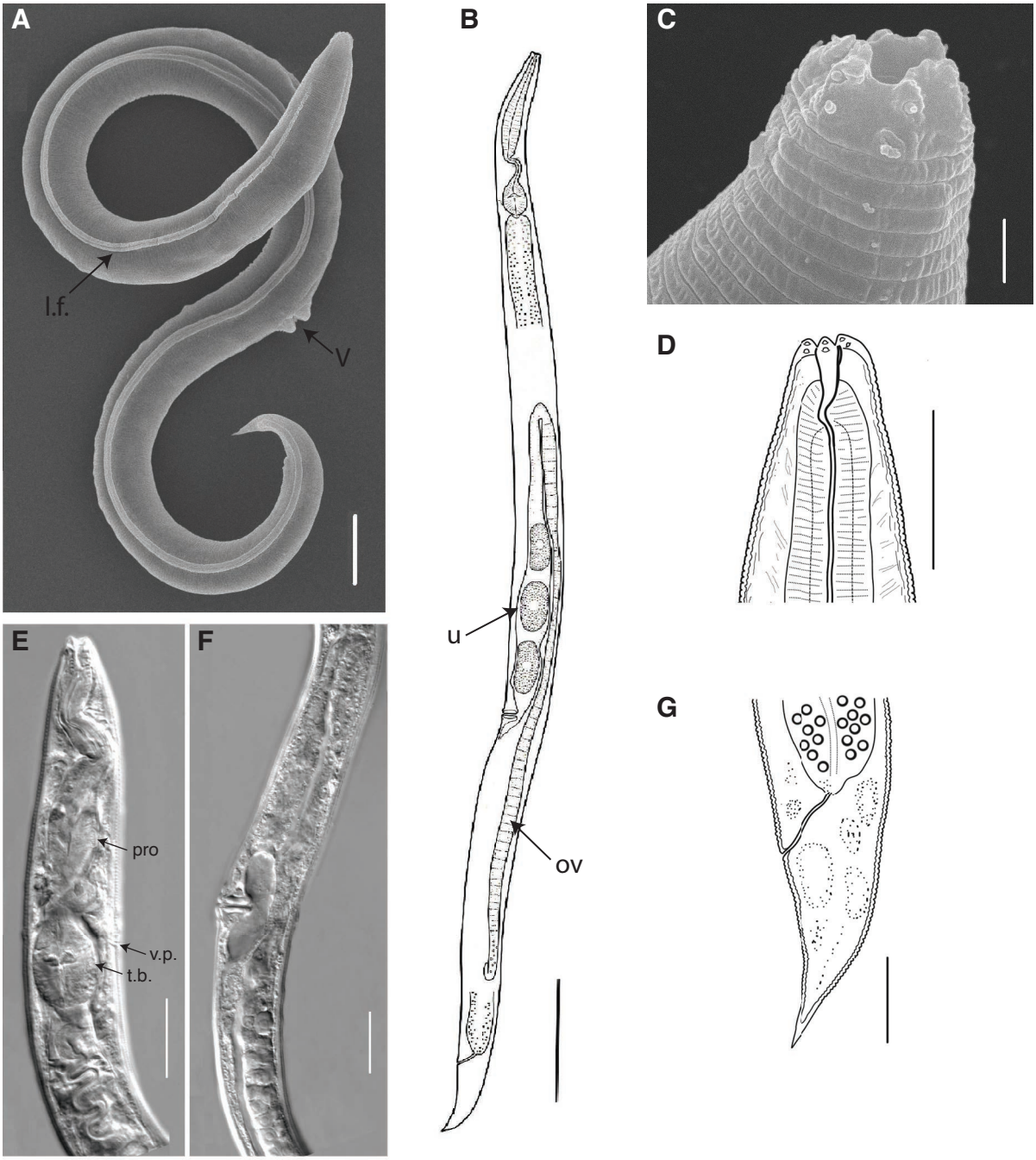

Figure 2
Shatilovich *et al*

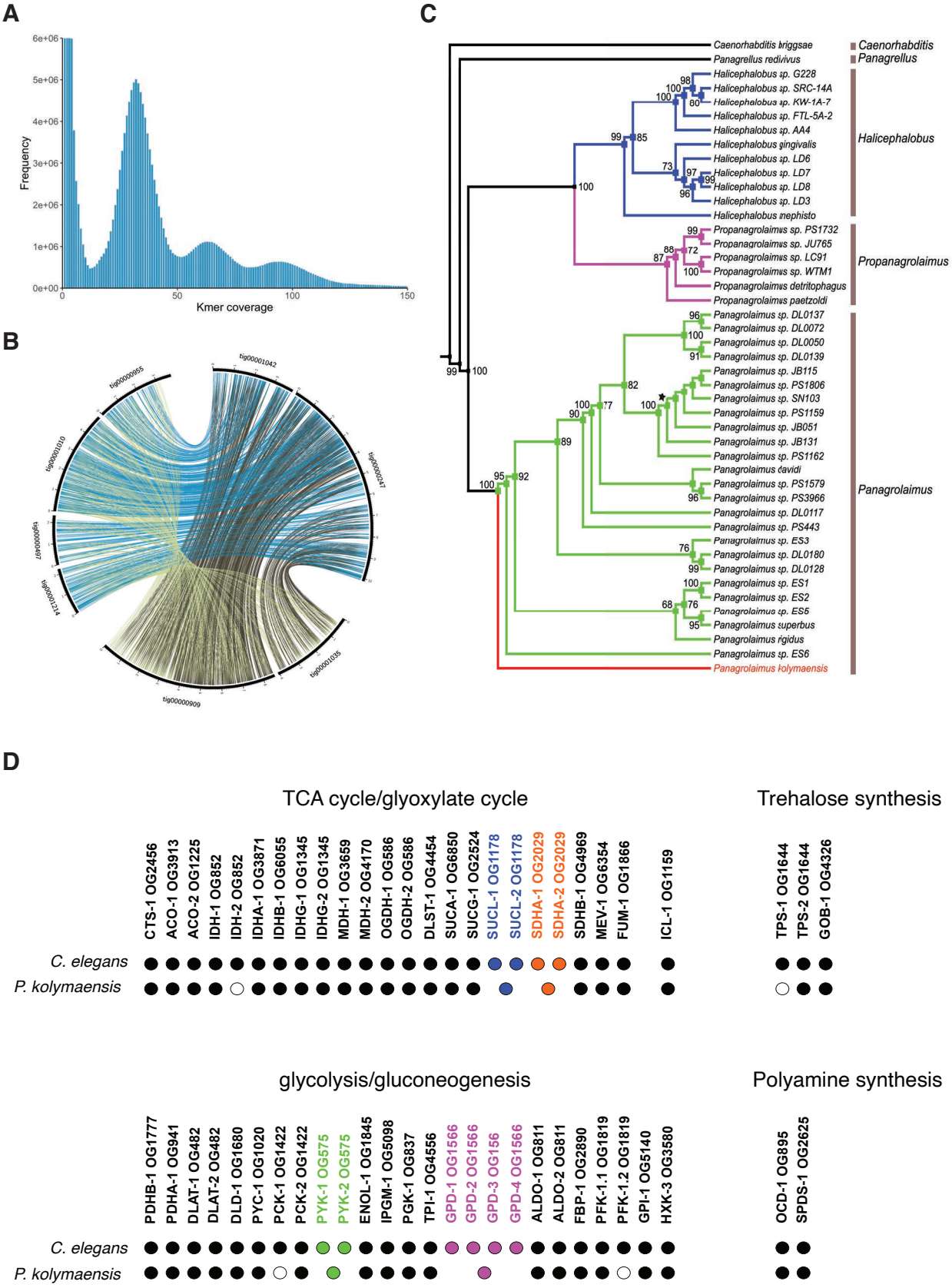

Figure 3
Shatilovich *et al*

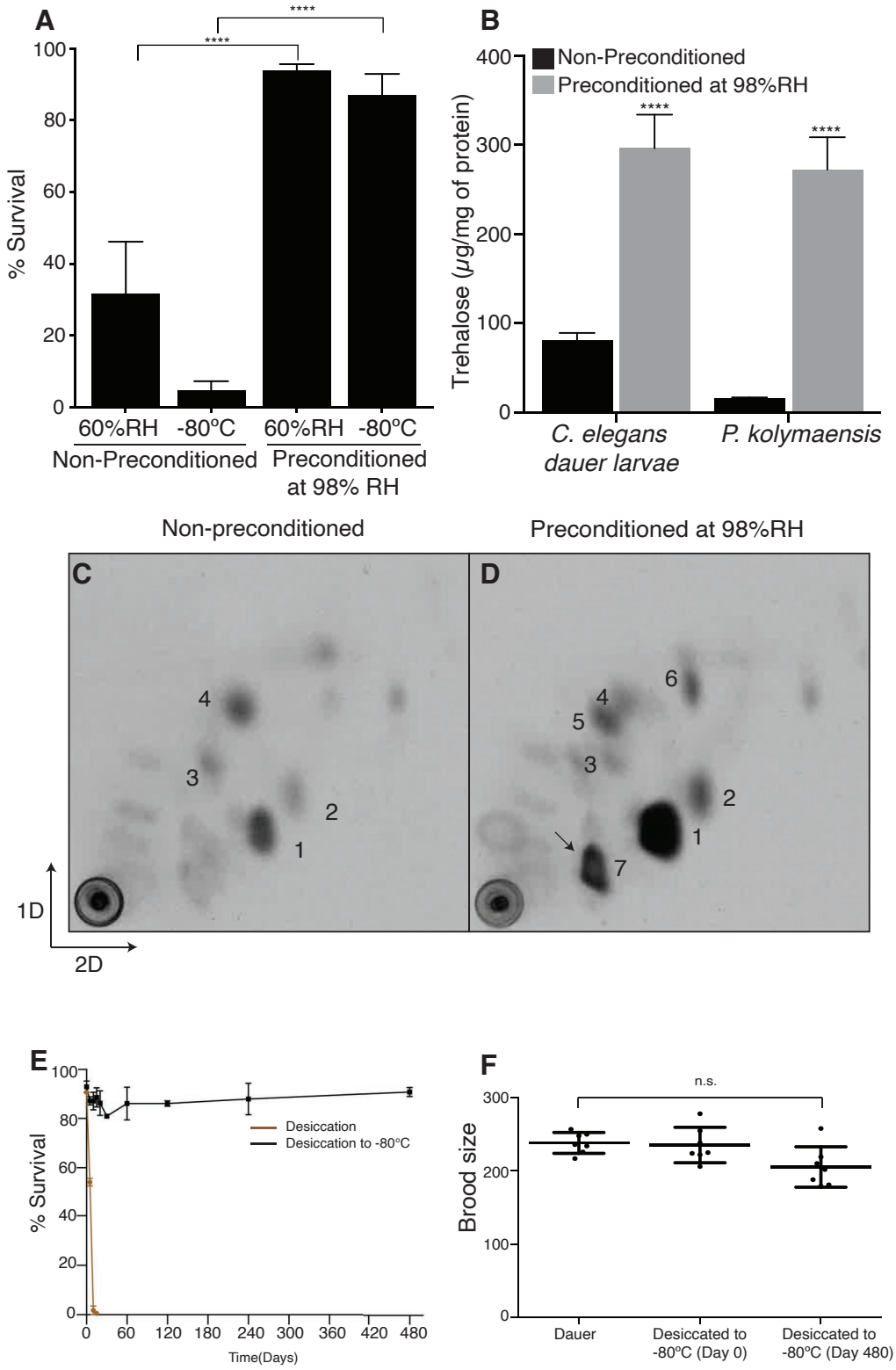

Figure 4
Shatilovich *et al*

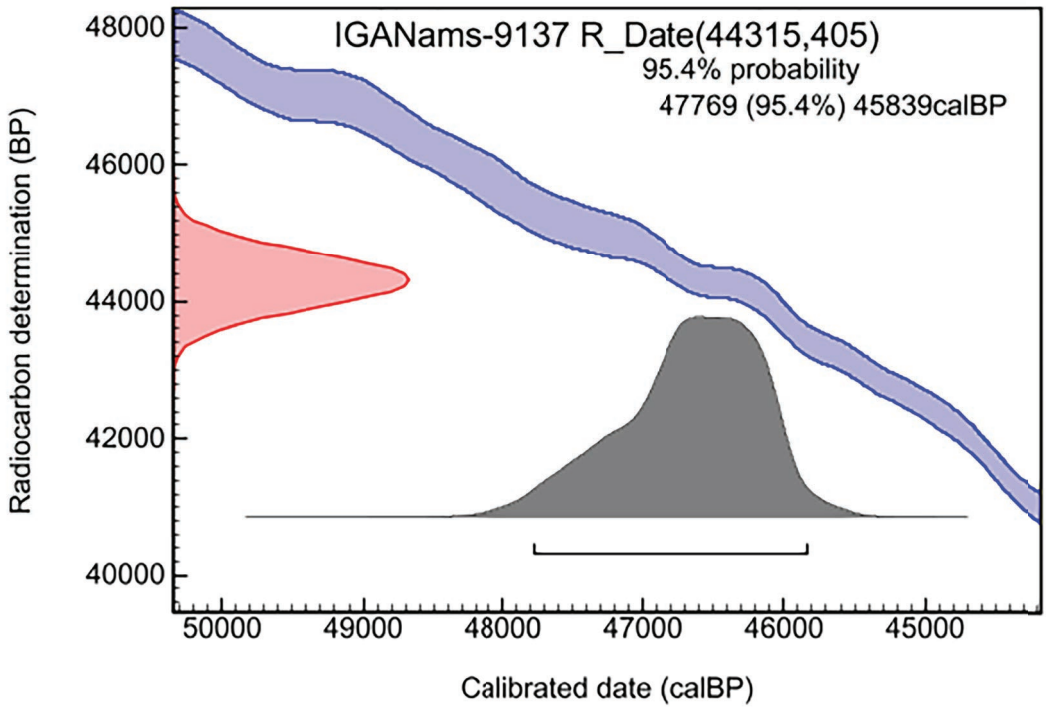

Figure S1
Shatilovich *et al*

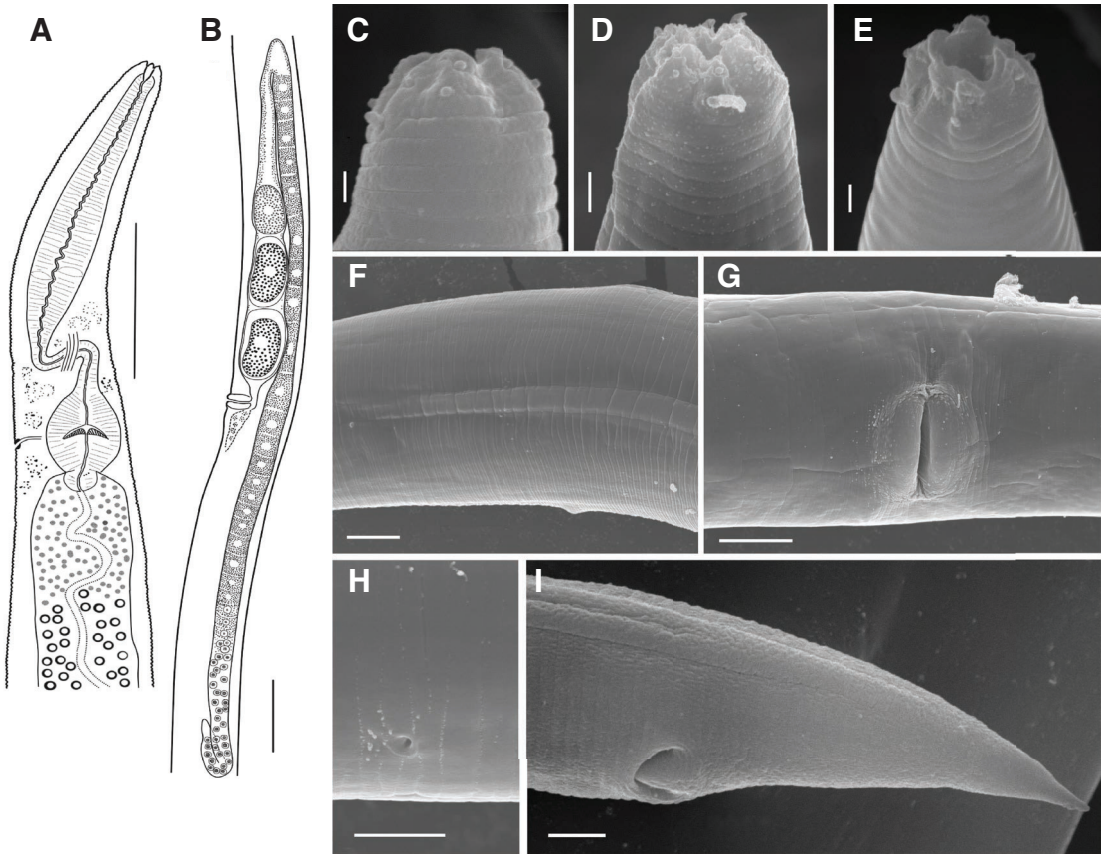

Figure S2
Shatilovich *et al*

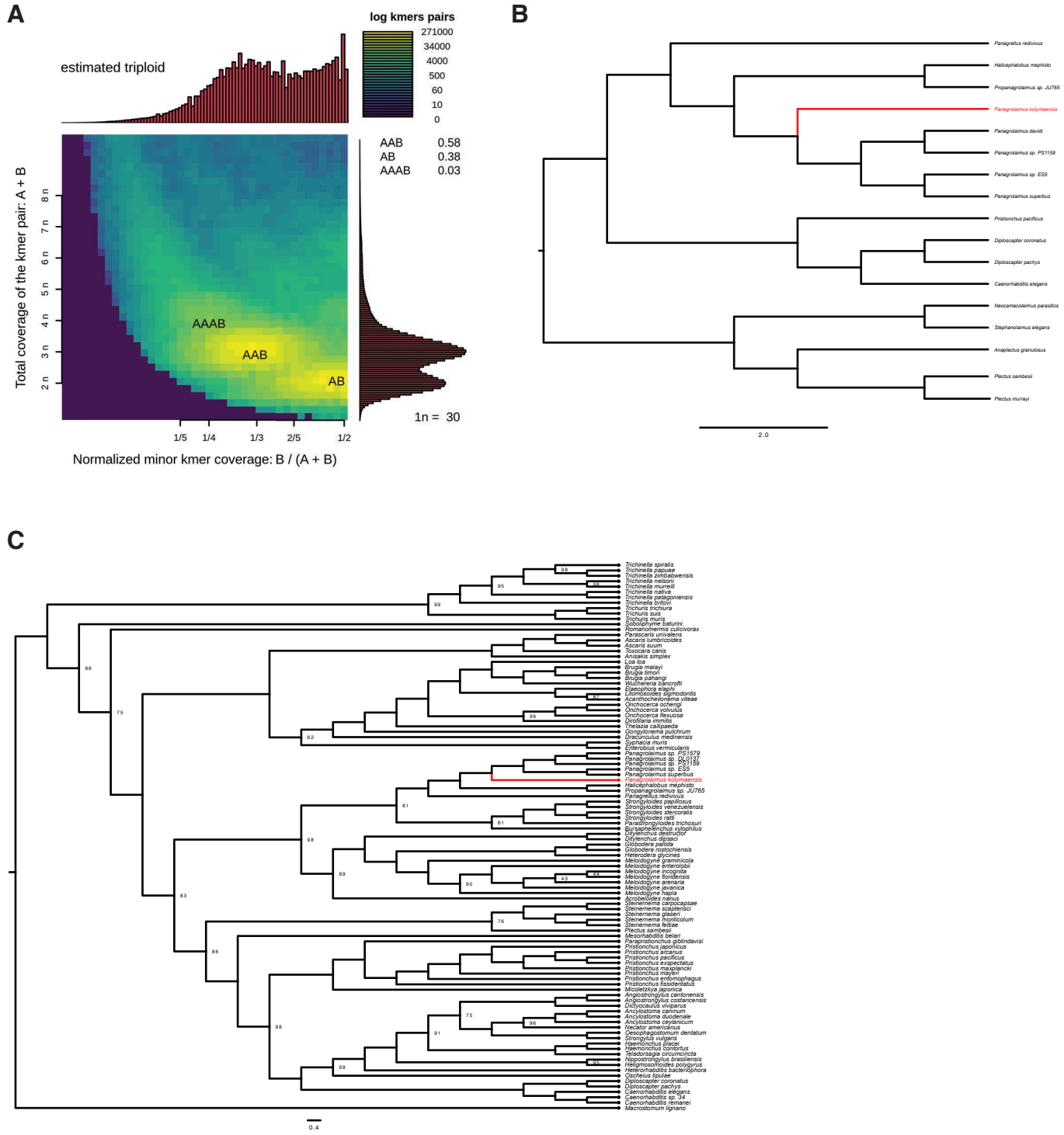

Figure S3
Shatilovich *et al*

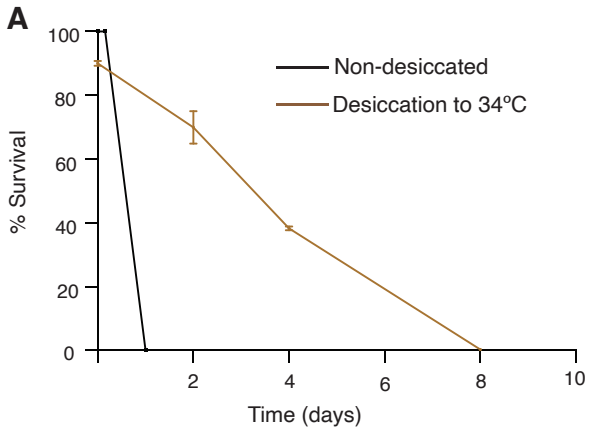

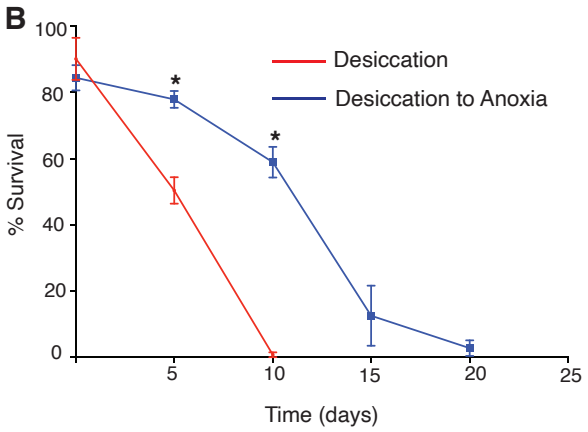

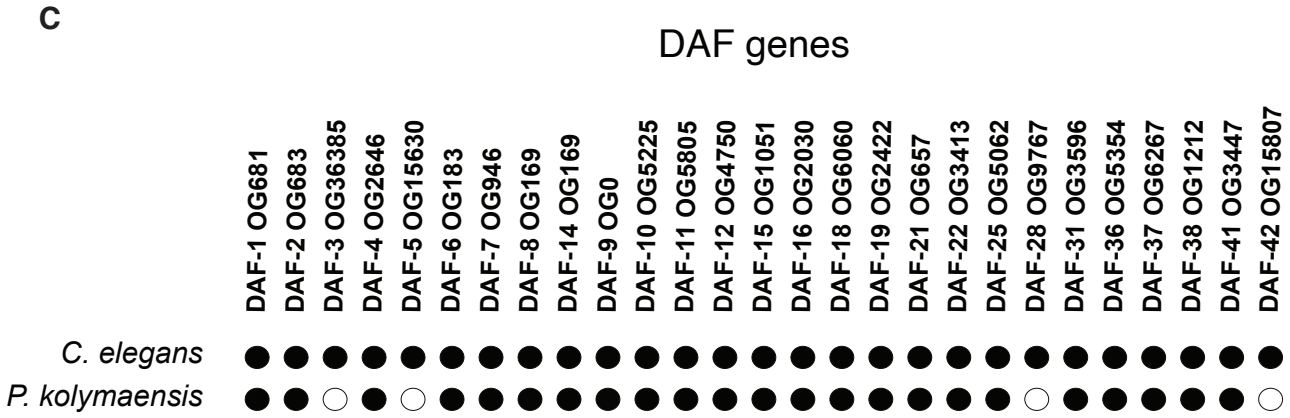

Figure S4
Shatilovich *et al*

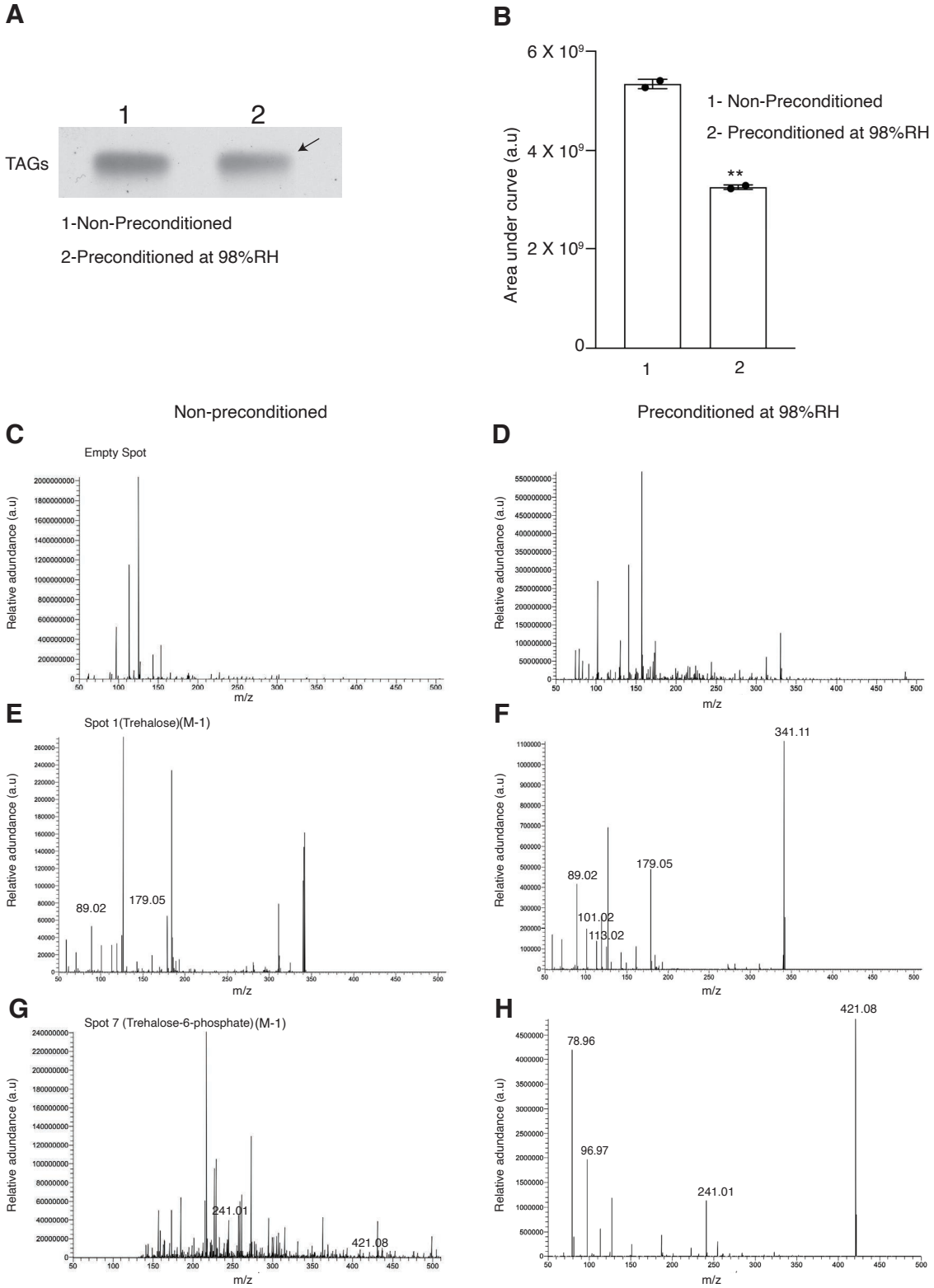

Figure S5
Shatilovich *et al*

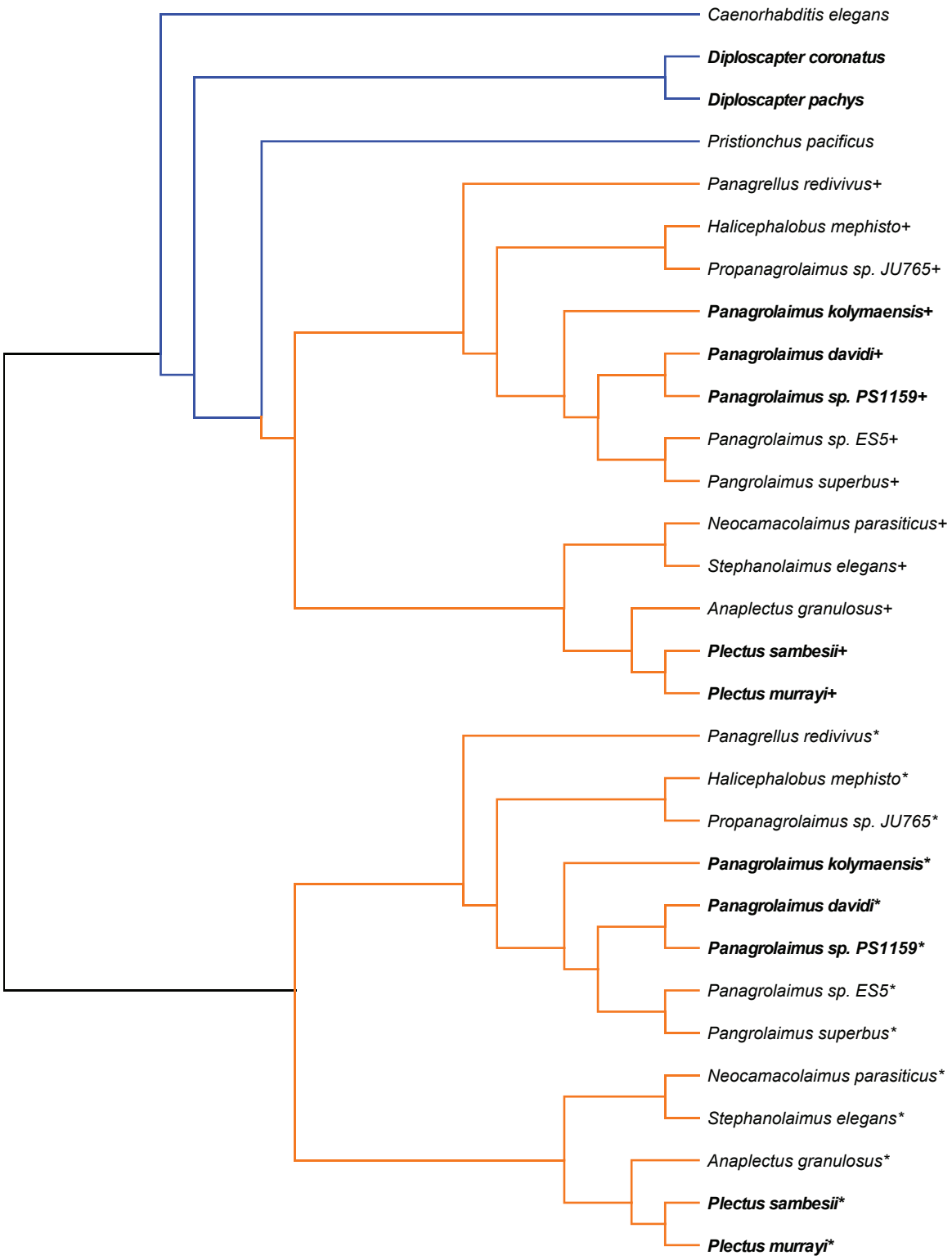

Figure S6
Shatilovich *et al*